Available online at www.sciencedirect.com
ScienceDirect
Trans. Nonferrous Met. Soc. China 21(2011) 1092−1104
Transactions of Nonferrous Metals Society of China
www.tnmsc.cn

Characteristic atom occupation patterns of Au_3Cu, $AuCu_3$, AuCuI and AuCuII based on experimental data of disordered alloys

XIE You-qing[1, 2, 3], LI Yan-fen[1, 2, 3], LIU Xin-bi[1, 2, 3], LI Xiao-bo[4], PENG Hong-jian[1, 2, 3], NIE Yao-zhuang[1, 2, 3]

1. School of Materials Science and Engineering, Central South University, Changsha 410083, China;
2. Powder Metallurgy Research Institute, Central South University, Changsha 410083, China;
3. State Key Laboratory for Powder Metallurgy, Central South University, Changsha 410083, China;
4. College of Mechanical Engineering, Xiangtan University, Xiangtan 411105, China

Received 14 April 2010; accepted 10 March 2011

Abstract: The potential energies, volumes and electronic structures of characteristic atoms coordinated by neighboring configurations were obtained from the experimental heats of formation and lattice parameters of disordered $Au_{1-x}Cu_x$ alloys. From characteristic atom occupation (CAO) patterns of $L1_2$-Au_3Cu, $L1_2$-$AuCu_3$ and $L1_0$-AuCu compounds, their electronic structures, volumetric and energetic properties were calculated. The CAO pattern of Johasson−Linde(J−L) model shows that the transition AuCuI→AuCuII is an exothermic and volume contraction reaction, which is opposite from experimental phenomena. According to CAO pattern of Guymont−Feutelais−Legendre(G−F−L) model, the AuCuII cell consists of two periodic antidirection (PAD) AuCuI regions and two PAD boundary regions. The equations derived from CAO pattern of G−F−L model can be used to calculate energetic properties, volumetric properties and ordering degrees of the PAD AuCuI region and PAD boundary region, as well as corresponding average properties of the AuCuII phase. The results are consistent with experimental phenomena.
Key words: Au-Cu system; intermetallics; electronic structure; crystalline structure; characteristic atom occupation pattern

1 Introduction

An alloy system contains three structure levels: phase level of organizations, atomic level of phases and electronic level of atoms. In order to get an entirely understanding of the alloy systems, to establish phase diagrams and to search a method for designing of alloys, the systematic science of alloys (SSA) has been established[1−5].

One of the main philosophic viewpoints in the SSA framework is that "A diversity of structures, properties and features of matter or non-matter systems should be attributed to combination and arrangement of structural units in the structural unit sequence". For example, the diversity of atoms in the atomic system is attributed to arrangement of electrons in the electronic orbital sequence; the diversity of substances in the matter system is attributed to composition of elements in the periodic sequence of elements; the diversity of geometric figures in the geometry is attributed to connection of straight lines in the straight line sequence with various lengths and curved lines in round sequence with various curvature radii; the diversity of species in the biological system is attributed to splice of the genes in the gene sequence; the diversity of music compositions in the music system is attributed to combination and arrangement of notes in the music note sequence.

In the fcc-based lattice Au-Cu system, each atom is coordinated by a nearest configuration [(*I*−*i*)Au, *i*Cu], where *i* denotes the number of Cu atoms and *I* is coordination number and equal to 12. In the $L1_0$-AuCu compound, each Au atom is coordinated by configuration [4Au, 8Cu], and named as A_8^{Au} characteristic atom; each Cu atom is coordinated by configuration [8Au, 4Cu], and named as A_4^{Cu} characteristic atom. Each characteristic atom has its own characters: potential energy, volume and electronic structure.

The crystalline structure of $L1_0$-AuCu compound can be described by combination of two superlattices, of

Foundation item: Project (50711181) supported by the National Natural Science Foundation of China; Project (2009FJ4016) supported by Natural Science Foundation of Hunan Province, China
Corresponding author: XIE You-qing; Tel: +86-731-88879287; E-mail: xieyouq2000@yahoo.com.cn
DOI: 10.1016/S1003-6326(11)60827-3

which one is occupied by A_8^{Au} atoms, another is occupied by A_4^{Cu} atoms. When $L1_0$-AuCu disorders to form the random $Au_{0.5}Cu_{0.5}$ alloy, the A_8^{Au} and A_4^{Cu} atoms are split, respectively, into the A_i^{Au} and A_i^{Cu} characteristic atom sequences, of which the concentrations x_i^{Au} and x_i^{Cu} can be calculated[3]. According to this basic analysis, three interconnected models have been provided for constructing diversity of structures and properties of alloy phases[5−8]:

1) The basic cluster overlapping (BCO) model. The structural units are a pair of basic cluster sequences, the first and second neighbor configurations and each cluster consists of a central atom.

2) The characteristic atom arranging (CAA) model. The structural units are a pair of characteristic atom sequences, and each characteristic atom is the central atom of a specific basic cluster.

3) The characteristic crystal mixing (CCM) model. The structure units are a pair of factitious characteristic crystal sequences, and each characteristic crystal consists of the same characteristic atoms with the identical potential energy, identical volume and identical electronic structure.

These three interconnected models were proposed in order to overcome disappointments of the atomic pair interaction model and central atom model[9], four-sublattice model and effective cluster interaction model[10−14].

One of the main methods in the SSA framework is that "the whole can be reproduced from a few parts" So the whole of a tree can be reproduced respectively from a seed, a leaf or a branch of the tree, and the whole of a sheep can be reproduced respectively from an egg cell or a body cell of the sheep in biologic systems; the whole information of an alloy system can be reproduced from information of a few disordered alloys or a few intermetallics, which may be obtained by experimental measurements or the first-principle calculations. This means that "the total potential energies and total volumes of a few alloys can be separated into the potential energy sequence and volume sequence of the characteristic atoms, from which the whole information about details of energetic and volumetric properties, electronic and crystalline structures of all alloy phases, as well as phase diagram of the alloy system can be reproduced".

The Au-Cu system has an extensive history in modern time on the metallic materials science. It has been considered a good platform for nearly all theories of alloys and nearly all experimental techniques to study electronic and crystalline structures of phases, order-disorder phase transformation and phase diagram. The SSA framework differs from previous theories mainly on two aspects: 1) it is established explicitly based on the philosophic viewpoints and methods; 2) the potential energies and volumes of characteristic atom sequences can be separated out from the total energy and total volume of alloy phase. The previous theories are the framework of total energy and total volume, which cannot be separated. Now, it is also used as the platform systematically to present the SSA framework through a series of papers. In the next section the main equations concerning with this paper are presented. According to the potential energies and volumes of characteristic atom sequences, the electronic structures, lattice constants, cohesive energies, potential energy curves and Debye temperatures of characteristic crystal sequences have been obtained by valence bond(VB) theory. According to the CAO patterns of the crystalline structures of observed $L1_2$-Au_3Cu, $L1_0$-AuCu and $L1_2$-$AuCu_3$ compounds, the obtained electronic structures and details of energetic and volumetric properties of these compounds are presented. According to the CAO patterns of the crystalline structures described by two models of the equiatomic AuCuII, the calculated volumetric properties, energetic properties and ordering degrees of AuCuII phase and its periodic antidirection(PAD) boundary region are shown.

2 Main equations

2.1 ε- and v-functions of characteristic atom sequences

Only considering the influence of the nearest neighboring configuration [(I−i)Au, iCu] on the central characteristic atoms, the potential energy ε-function and volume V-function of characteristic atom sequences are obtained[15−17]:

$$\begin{cases}\varepsilon_i^{Au}=\varepsilon_0^{Au}+(i/I)^2(\varepsilon_I^{Au}-\varepsilon_0^{Au})\\ \varepsilon_i^{Cu}=\varepsilon_I^{Cu}+[(I-i)/I]^2(\varepsilon_0^{Cu}-\varepsilon_I^{Cu})\end{cases} \tag{1}$$

$$\begin{cases}v_i^{Au}=v_0^{Au}+(i/I)^2(v_I^{Au}-v_0^{Au})\\ v_i^{Cu}=v_I^{Cu}+[2(I-i)/I](v_0^{Cu}-v_I^{Cu})-\\ \qquad [(I-i)/I]^2(v_0^{Cu}-v_I^{Cu})\end{cases} \tag{2}$$

When considering influence of the first and second neighboring configuration {[(I−i)Au, iCu], [(J−j)Au, jCu]}, the ε- and V-functions can be modified as follows:

$$\begin{cases}\varepsilon_{i,j}^{Au}=\varepsilon_{0,0}^{Au}+[(i+j/J)/I]^2(\varepsilon_{I,0}^{Au}-\varepsilon_{0,0}^{Au})\\ \varepsilon_{i,j}^{Cu}=\varepsilon_{I,J}^{Cu}+[(I-i+(J-j)/J)/I]^2(\varepsilon_{0,J}^{Cu}-\varepsilon_{I,J}^{Cu})\end{cases} \tag{3}$$

$$\begin{cases}v_{i,j}^{Au}=v_{0,0}^{Au}+[(i+j/J)/I]^2(v_{I,0}^{Au}-v_{0,0}^{Au})\\ v_{i,j}^{Cu}=v_{I,J}^{Cu}+\{[2(I-i+(J-j)/J)/I]-\\ \qquad [(I-i+(J-j)/J)/I]^2\}(v_{0,J}^{Cu}-v_{I,J}^{Cu})\end{cases} \tag{4}$$

where, J=6; j is the number of Cu atoms in the second neighboring configuration. $\varepsilon_{0,0}^{\mathrm{Au}}=\varepsilon_0^{\mathrm{Au}}$, $\varepsilon_{I,0}^{\mathrm{Au}}=\varepsilon_I^{\mathrm{Au}}$, $v_{0,0}^{\mathrm{Au}}=v_0^{\mathrm{Au}}$, $v_{I,0}^{\mathrm{Au}}=v_I^{\mathrm{Au}}$, $\varepsilon_{I,J}^{\mathrm{Cu}}=\varepsilon_I^{\mathrm{Cu}}$, $\varepsilon_{0,J}^{\mathrm{Cu}}=\varepsilon_0^{\mathrm{Cu}}$, $v_{I,J}^{\mathrm{Cu}}=v_I^{\mathrm{Cu}}$, $v_{0,J}^{\mathrm{Cu}}=v_0^{\mathrm{Cu}}$.

2.2 Description for electronic structures of characteristic crystals

In the valence bond (VB) theory, the electronic structure of a characteristic crystal, i.e. characteristic atom, is illustrated by valence electrons of one-atom state ψ hybridized by several basic atom states in the basic atom state ϕ_k sequence:

$$\psi=\sum_k c_k\phi_k \tag{5}$$

The hybridized composition c_k can be found from combination of three basic states (see section 3.1.2).

If s_k^{c}, p_k^{c} and d_k^{c} denote respectively the numbers of covalent electrons of s, p and d orbitals in the k basic atom state; d_k^{n}, s_k^{f} and p_k^{f} denote respectively the number of non-valence d electrons, free s and p electrons, from which the OEO numbers of the characteristic crystal can be obtained by following expressions:

$$\begin{aligned}
&s_{\mathrm{c}}=\sum_k c_k s_k^{\mathrm{c}},\ p_{\mathrm{c}}=\sum_k c_k p_k^{\mathrm{c}},\ d_{\mathrm{c}}=\sum_k c_k d_k^{\mathrm{c}},\\
&s_{\mathrm{f}}=\sum_{\mathrm{k}} c_k s_k^{\mathrm{f}},\ p_{\mathrm{f}}=\sum_k c_k p_k^{\mathrm{f}},\ n_{\mathrm{c}}=s_{\mathrm{c}}+p_{\mathrm{c}}+d_{\mathrm{c}},\\
&n_{\mathrm{f}}=s_{\mathrm{f}}+p_{\mathrm{f}},\ n_{\mathrm{v}}=n_{\mathrm{c}}+n_{\mathrm{f}},\ R=\sum_k c_k R_k,\ \sum_k c_k=1
\end{aligned} \tag{6}$$

where R_k, which is the single bond radius, can be obtained from Pauling's equation[18] slightly modified[19−20]:

$$\begin{cases}
R_k^{\mathrm{Au}}=1.5150-0.2522\delta_k\\
R_k^{\mathrm{Cu}}=1.3474-0.2492\delta_k\\
\delta_k=d_k^{\mathrm{c}}/n_{\mathrm{v}}
\end{cases} \tag{7}$$

2.3 Bond length and lattice constant equations

Pauling's bond length equation should be suitable to various bonds in the characteristic crystal, we have (in nm):

$$\begin{cases}
r_s=2R-\beta\lg n_s\\
n_{\mathrm{c}}=\sum_s I_s n_s
\end{cases} \tag{8}$$

where s=1, 2 and 3; r_1, r_2, r_3 and I_1, I_2, I_3 denote respectively the length values and the numbers of the first, second and third neighboring bonds; n_1, n_2 and n_3 denote respectively the numbers of pairs of covalent electrons on the relative bonds; β is Pauling's coefficient[18].

For a fcc crystal, the lattice constant equation can be derived from Eq.(8)[21−22]:

$$a=\frac{1}{G_1}\left[2R(1)-\beta\lg\frac{n_{\mathrm{c}}}{\sum_s I_s\times10^{(G_1-G_s)a/\beta}}\right] \tag{9}$$

where s=1, 2, 3; $G_1=\sqrt{2}/2$, G_2=1, $G_3=\sqrt{6}/2$; n_{c} is obtained by Eq.(6). It is a convergent transcendental function of the lattice constant.

2.4 Cohesive energy equation and MAI potential function

Considering contributions of the covalent and near free electrons to cohesive energy, the cohesive energy equation (E_{c}) and potential function ($w(r)$) with many-atom interactions (MAI) of characteristic crystals have been established[23] , which are (in kJ/mol):

$$E_{\mathrm{c}}=\frac{314}{n'-0.36g}\left[\sum\frac{I_s n_s}{r_{s,0}}f+\frac{n_f}{\bar{r}_s}f'\right] \tag{10}$$

$$w(r)=E_{\mathrm{c}}[-n(\frac{r_0}{r})^x+(n-1)(\frac{r_0}{r})^{nx/(n-1)}] \tag{11}$$

where

$$\begin{aligned}
&f=\sqrt{\alpha}+\sqrt{3\beta}+\sqrt{5\gamma},\\
&\alpha=s_{\mathrm{c}}/n_v,\quad \beta=p_{\mathrm{c}}/n_v,\quad \gamma=d_{\mathrm{c}}/n_v,\\
&f'=\sqrt{2\alpha'},\alpha'=n_{\mathrm{f}}/n_v,\quad \bar{r}_s=(\sum_s I_s r_s)/\sum_s I_s
\end{aligned} \tag{12}$$

r_0 and r may denote any kind of bond length, but in the present work, they express the shortest lengths of the crystal in equilibrium and nonequilibrium, respectively; f and f' are respectively the bonding capacities of the hybrid covalent electrons and near free electrons. The constants n' and g should be taken respectively as 4 and 1 for Au and Cu elements.

The exponent x in the MAI potential function is obtained by Debye theory[22−23].

$$x^2=4\theta^2k_{\mathrm{B}}^2r_0^2m(n-1)/n\hbar^2j^2E_{\mathrm{c}} \tag{13}$$

where θ is Debye temperature; k_{B} is the Boltzman's constant; $\hbar$ is the Planck's constant; m is atomic mass; j and n are respectively the multiple of the half cutoff wave length and another exponent of the MAI potential function, which can be obtained from two experimental values of the linear thermal expansion coefficients at two temperatures.

The Debye temperature θ_i^α of the C_i^α-characteristic crystal is approximately obtained by following equation.

$$\theta_i^\alpha=\theta_\alpha^0\sqrt{E_i^\alpha/(V_i^\alpha)^{2/3}}/\sqrt{E_\alpha^0/(V_\alpha^0)^{2/3}} \tag{14}$$

where E_α^0, V_α^0 and θ_α^0, as well as E_i^α and V_i^α are

respectively potential energy, volume and Debye temperature of the pure metal and C_i^{α} -characteristic crystal of α-component at 0 K.

2.5 Additive law of characteristic atoms and volume mismatch

The intermetallic compounds can be thought to be formed by arranging characteristic atoms. When considering the influence of the first and second neighbor configurations {[(*I*−*i*)Au, *i*Cu], [(*J*−*j*)Au, *j*Cu]}, the total state ψ, total potential energy E and total volume V of a cell for compounds can be obtained by the additive law of characteristic atoms (simplified as CAA-law):

$$\begin{cases} \psi = \sum\limits_{\alpha=\mathrm{Au,Cu}} \sum\limits_{i=0}^{I=12} \sum\limits_{j=0}^{J=6} (n_{i,j}^{\alpha} \psi_{i,j}^{\alpha}) \\ E = \sum\limits_{\alpha=\mathrm{Au,Cu}} \sum\limits_{i=0}^{I=12} \sum\limits_{j=0}^{J=6} (n_{i,j}^{\alpha} \varepsilon_{i,j}^{\alpha}) \\ V = \sum\limits_{\alpha=\mathrm{Au,Cu}} \sum\limits_{i=0}^{I=12} \sum\limits_{j=0}^{J=6} (n_{i,j}^{\alpha} V_{i,j}^{\alpha}) \end{cases} \tag{15}$$

The average atomic volume mismatch degree between characteristic atoms inside α component is

$$\begin{cases} \Delta m_v^{\alpha} = \sum\limits_i \sum\limits_j n_{i,j}^{\alpha} \left| (V_{i,j}^{\alpha} - v_a^{\alpha}) \right| / \sum\limits_i \sum\limits_j n_{i,j}^{\alpha} v_a^{\alpha} \\ v_a^{\alpha} = \sum\limits_i \sum\limits_j n_{i,j}^{\alpha} V_{i,j}^{\alpha} / \sum\limits_i \sum\limits_j n_{i,j}^{\alpha} \end{cases} \tag{16}$$

The average atomic volume mismatch degree between components Au and Cu is

$$\begin{cases} \Delta m_V = \sum\limits_{\alpha} \sum\limits_i \sum\limits_j n_{i,j}^{\alpha} \left| V_{i,j}^{\alpha} - v_a \right| / \sum\limits_{\alpha} \sum\limits_i \sum\limits_j n_{i,j}^{\alpha} v_a \\ v_a = \sum\limits_{\alpha} \sum\limits_i \sum\limits_j n_{i,j}^{\alpha} V_{i,j}^{\alpha} / \sum\limits_{\alpha} \sum\limits_i \sum\limits_j n_{i,j}^{\alpha} \end{cases} \tag{17}$$

The total average atomic volume mismatch degree of a compound is

$$\Delta m_V^{\mathrm{T}} = \Delta m_V + \sum_{\alpha} (n_{\alpha} / n_T) \Delta m_V^{\alpha} \tag{18}$$

In Eqs.(15)−(18), $\psi_{i,j}^{\alpha}$, $\varepsilon_{i,j}^{\alpha}$, $V_{i,j}^{\alpha}$ and $n_{i,j}^{\alpha}$ are, respectively, electronic structure, potential energy, volume and number of the $A_{i,j}^{\alpha}$ characteristic atom in a cell; v_a^{α} is the average atomic volume of the α-component; n_{α} and n_{T} are respectively the number of atoms of the α-component and total number of atoms in a cell; v_a is the average atomic volume of the compound.

In a similar way to obtain various volume mismatch degrees, we can obtain corresponding potential energy mismatch degree: $\Delta m_{\varepsilon}^{\alpha}$, Δm_{ε}, $\Delta m_{\varepsilon}^{\mathrm{T}}$.

3 Results

3.1 Structures and properties of characteristic crystals (atoms)

3.1.1 Basic atomic states and corresponding fcc-crystals

According to covalent electron number (d_{c}, s_{c}), free electron number (s_{f}, p_{f}) and non-valence electron number (d_{n}) in outer shell of a basic state atom, the single bond radius (R), lattice constant (a) and cohesive energy (E_{c}) of fcc-crystals formed respectively by the same Au and the same Cu basic state (ϕ) atoms can be calculated by Eqs.(6)−(13). Table 1 shows these results of some basic states.

3.1.2 Electronic structures of characteristic crystals

The precise solution (hybridized composition) of electronic structure of each characteristic crystal can be found from combination of three basic states, through the cross point of the equilattice constant a-line and equicohesive energy E_{c}-line of this characteristic crystal. The solutions of electronic structures of primary C_0^{Au} and C_{12}^{Cu} characteristic crystals are shown in Fig.1.

The electronic structures of pure Au and Cu metals, i.e. primary characteristic crystals, were also calculated from linear muffintin-tin orbitals(LMTO) method in the energy band (EB) theory by us and were calculated from linear rigorous cell (LRC) method by ECKARDT et

Table 1 Some Au and Cu basic atomic states in Au and Cu basic atom state sequences and corresponding fcc-crystals

ϕ_n	Electron in outer shell					Au-crystal			Cu-crystal		
	d_{n}	d_{c}	s_{c}	s_{f}	p_{f}	R/Å	a/Å	E_{c}/(kJ·mol^{-1})	R/Å	a/Å	E_{c}/(kJ·mol^{-1})
1	0	9	0	1	1	1.308 7	3.828 8	603.44	1.143 6	3.362 7	685.33
2	0	9	1	1	0	1.308 7	3.788 4	753.69	1.143 6	3.326 3	855.19
3	4	5	0	1	1	1.334 9	4.100 2	311.11	1.169 4	3.633 9	350.6
4	4	6	0	1	0	1.298 8	3.931 6	395.84	1.133 8	3.466 9	448.16
5	6	3	0	1	1	1.363 7	4.465 2	174.68	1.197 9	3.998 6	194.8
6	6	3	1	1	0	1.363 7	4.263 6	261.33	1.197 9	3.796 0	293.21
7	6	4	0	1	0	1.313 3	4.121 3	249.09	1.148 1	3.655 6	280.47
8	8	1	0	1	1	1.430 9	5.132 7	67.797	1.264 4	4.662 7	74.604

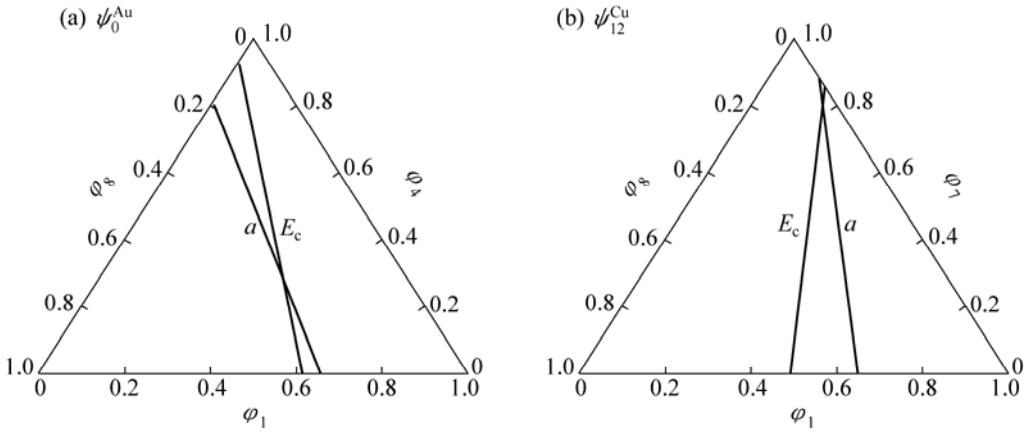

Fig.1 Hybridized compositions of basic states and electronic structures for primary C_0^{Au} and C_{12}^{Cu} characteristic crystals at 0 K: (a) $\psi_0^{Au}=0.4464\varphi_1+0.2557\varphi_4+0.2979\varphi_8=[Xe](5d_n)^{3.4060}(5d_c)^{5.8497}(6s_f+6p_f)^{1.7443}=[Xe](5d)^{9.2567}(6s)^{1.7443}$; (b) $\psi_{12}^{Cu}=0.1627\varphi_1+0.8075\varphi_7+0.0298\varphi_8=[Ar](3d_n)^{5.0833}(3d_c)^{4.7241}(4s_f+4P_f)^{1.1926}=[Ar](3d)^{9.8074}(4s)^{1.1926}$ ([Xe] is Xenon electronic structure; [Ar] is Argon electronic structure)

al[24]. In their opinion: "as a result of the strong s-p hybridization the occupation of the formerly unoccupied p level becomes practically equal to that of the s level". These results are approaching to ones by VB theory:

$$\begin{cases}\psi_0^{Au}(\text{LRC})=[Xe](5d)^{9.464}(6s)^{0.772}(6p)^{0.764}=\\ \qquad [Xe](5d)^{9.464}(6s)^{1.536}\\ \psi_0^{Au}(\text{LMTO})=[Xe](5d)^{9.64}(6s)^{0.76}(6p)^{0.60}=\\ \qquad [Xe](5d)^{9.64}(6s)^{1.36}\end{cases}$$

$$\begin{cases}\psi_{12}^{Cu}(\text{LRC})=[Ar](3d)^{9.645}(4s)^{0.671}(4p)^{0.684}=\\ \qquad [Ar](3d)^{9.645}(4s)^{1.355}\\ \psi_{12}^{Cu}(\text{LMTO})=[AE](3d)^{9.70}(4s)^{0.52}(4p)^{0.78}=\\ \qquad [Ar](3d)^{9.70}(4s)^{1.30}\end{cases}$$

The lattice constants and cohesive energies calculated from LMTO method are respectively 0.403 9 nm and 438 kJ/mol for fcc pure Au metal and 0.355 1 nm and 419.19 kJ/mol for fcc pure Cu metal. These results are not in good agreement with experiments and not satisfied to calculate thermodynamic properties of alloys. According to electronic structures of primary C_0^{Au} and C_{12}^{Cu} characteristic crystals, their potential energy curves are calculated by Eqs.(8)−(11) and shown in Fig.2.

3.1.3 Characteristic crystal sequences

According to the potential energies and volumes of A_i^{Au} and A_i^{Cu} characteristic atoms, the electronic structures, single bond radii, cohesive energies and Debye temperatures of C_i^{Au} and C_i^{Cu} characteristic crystals have been calculated by VB theory and are listed in Table 2. The nature of variations in potential energies and volumes of A_i^{Au} and A_i^{Cu} characteristic atoms can be expounded.

1) For C_i^{Au} characteristic crystals, the atomic potential energy lowers with increasing the i number of Cu-atoms in the configuration [(I−i)Au, iCu], essentially due to both increase of total valence electrons $n_v=(d_c+s_c+s_f+p_f)$ and reduction of atomic volume; the atomic volume reduces, essentially due to both increase of total covalent electrons $n_c=(d_c+s_c)$ and

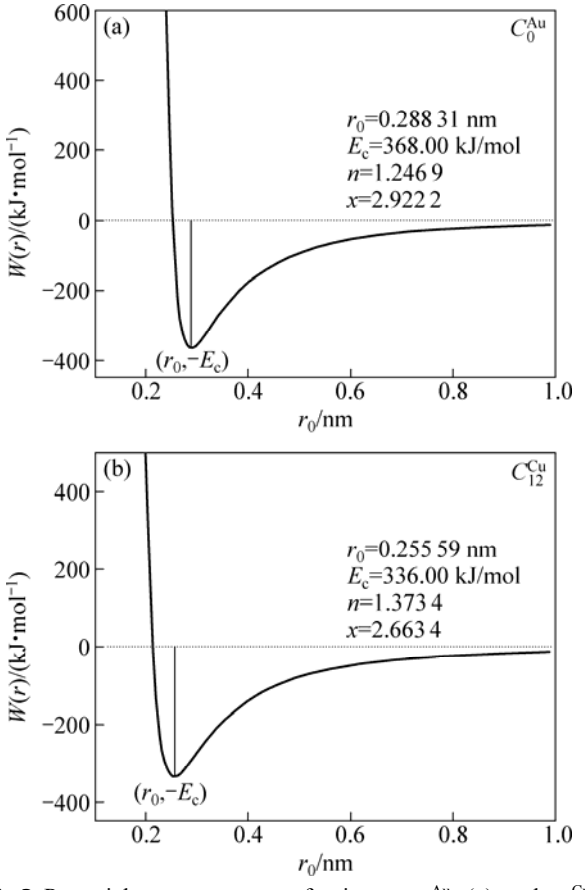

Fig.2 Potential energy curves of primary C_0^{Au} (a) and C_{12}^{Cu} (b) characteristic crystals at 0 K

Table 2 Valence electrons in outer shell, atomic potential energies (ε), atomic volumes (v), single bond radii (R), cohesive energies (E_c) and Debye temperatures (θ) of C_i^{Au} and C_i^{Cu} characteristic crystal sequences in Au-Cu system at 0 K

Crystal	C_i^{α}	Valence electrons in outer shell					v/Å^3	ε/ (eV·atom^{-1})	a/Å	R/Å	E_c/ (kJ·mol^{-1})	θ/K
		d_n	d_c	s_c	s_f	p_f						
	0	3.4060	5.8497	0	1	0.7443	16.7841	−3.8141	4.0643	1.3426	368.00	165.00
	1	3.4092	5.8508	0	1	0.7400	16.7742	−3.8158	4.0635	1.3423	368.16	165.07
	2	3.4168	5.8546	0	1	0.7286	16.7469	−3.8208	4.0613	1.3416	368.64	165.27
	3	3.4309	5.8607	0	1	0.7084	16.7000	−3.8291	4.0575	1.3404	369.45	165.60
	4	3.4507	5.8690	0	1	0.6803	16.6346	−3.8408	4.0522	1.3387	370.58	166.07
	5	3.4775	5.8793	0	1	0.6433	16.5498	−3.8558	4.0453	1.3365	372.03	166.68
Au	6	3.5114	5.8913	0	1	0.5972	16.4457	−3.8742	4.0368	1.3338	373.80	167.43
	7	3.5522	5.9050	0	1	0.5428	16.3238	−3.8959	4.0268	1.3305	375.90	168.31
	8	3.6022	5.9197	0	1	0.4781	16.1819	−3.9210	4.0151	1.3267	378.31	169.35
	9	3.6601	5.9354	0	1	0.4045	16.0228	−3.9494	4.0019	1.3224	381.05	170.52
	10	3.7299	5.9508	0	1	0.3193	15.8433	−3.9811	3.9869	1.3174	384.11	171.85
	11	3.8105	5.9659	0	1	0.2237	15.6462	−4.0162	3.9703	1.3118	387.50	173.32
	12	3.9052	5.9793	0	1	0.1154	15.4297	−4.0546	3.9519	1.3056	391.20	174.96
	0	3.9436	5.1340	0	1	0.9224	12.6653	−3.6649	3.7002	1.1964	353.61	342.56
	1	4.0121	5.0923	0	1	0.8955	12.6591	−3.6358	3.6996	1.1951	350.79	341.25
	2	4.0853	5.0522	0	1	0.8625	12.6386	−3.6092	3.6976	1.1934	348.23	340.19
	3	4.1631	5.0137	0	1	0.8232	12.6038	−3.5851	3.6942	1.1912	345.90	339.36
	4	4.2441	4.9770	0	1	0.7789	12.5568	−3.5635	3.6896	1.1886	343.83	338.76
	5	4.3305	4.9417	0	1	0.7278	12.4946	−3.5445	3.6835	1.1855	341.99	338.42
Cu	6	4.4197	4.9082	0	1	0.6722	12.4215	−3.5280	3.6763	1.1821	340.40	338.29
	7	4.5153	4.8756	0	1	0.6090	12.3325	−3.5141	3.6675	1.1781	339.06	338.43
	8	4.6163	4.8442	0	1	0.5394	12.2299	−3.5027	3.6573	1.1736	337.96	338.82
	9	4.7223	4.8138	0	1	0.4639	12.1149	−3.4938	3.6458	1.1687	337.10	339.46
	10	4.8350	4.7839	0	1	0.3810	11.9857	−3.4875	3.6328	1.1633	336.49	340.37
	11	4.9552	4.7542	0	1	0.2907	11.8428	−3.4837	3.6183	1.1573	336.12	341.55
	12	5.0833	4.7241	0	1	0.1926	11.6864	−3.4824	3.6023	1.1508	336.00	343.00

decrease of Pauling's single bond radius R, which is attributed to increase of $\delta = d_c / n_v$ (Eq.(7)).

2) For C_i^{Cu} characteristic crystals, the atomic potential energy lowers with increasing the (I−i) number of Au-atoms in the configuration [(I−i)Au, iCu], mainly due to the increase of total valence electrons, even the increase of the atomic volume rises; the atomic volume rises mainly due to the increase of Pauling's single bond radius R, which is attributed to decrease of $\delta = d_c / n_v$, even the increase of total covalence electrons.

According to the potential energies and volumes of $A_{i,j}^{Au}$ and $A_{i,j}^{Cu}$ characteristic atoms coordinated by configuration {[(I−i)Au, iCu], [(J−j)Au, jCu]}, the electronic structures and properties of $C_{i,j}^{Au}$ and $C_{i,j}^{Cu}$ characteristic crystals consisting of $A_{i,j}^{Au}$ and $A_{i,j}^{Cu}$ atoms are also calculated, but here these results are not listed.

In Table 1, $C_i^{Au} = C_{i,0}^{Au}$, $C_i^{Cu} = C_{i,6}^{Cu}$. The effect of the second neighboring configuration [(J−j)Au, jCu] on these properties can not be considered calculating variations of volumetric and energetic properties of alloys with composition and ordering degree.

3.2 $L1_2$-Au_3Cu, $L1_0$-AuCu and $L1_2$-$AuCu_3$ compounds

According to CAO patterns of observed $L1_2$-Au_3Cu, $L1_0$-AuCu and $L1_2$-$AuCu_3$ compounds, we can obtain electronic structures, potential energy wave planes, details of volumetric and energetic properties of these compounds (see Fig.3 and Table 3), from which the following information is obtained.

The electronic structures of $L1_2$-Au_3Cu, $L1_0$-AuCu and $L1_2$-$AuCu_3$ compounds are described by those of characteristic atoms (see Table 2):

$$\psi(Au_3Cu) = 3[Xe](5d_n)^{3.4507}(5d_c)^{5.8690}(6s_f)^{1.6803} + [Ar](3d_n)^{3.9436}(3d_c)^{5.1340}(4s_f)^{1.9224}$$

$$\psi(AuCu) = [Xe](5d_n)^{3.6022}(5d_c)^{5.9197}(6s_f)^{1.4781} + [Ar](3d_n)^{4.2441}(3d_c)^{4.9770}(4s_f)^{1.7789}$$

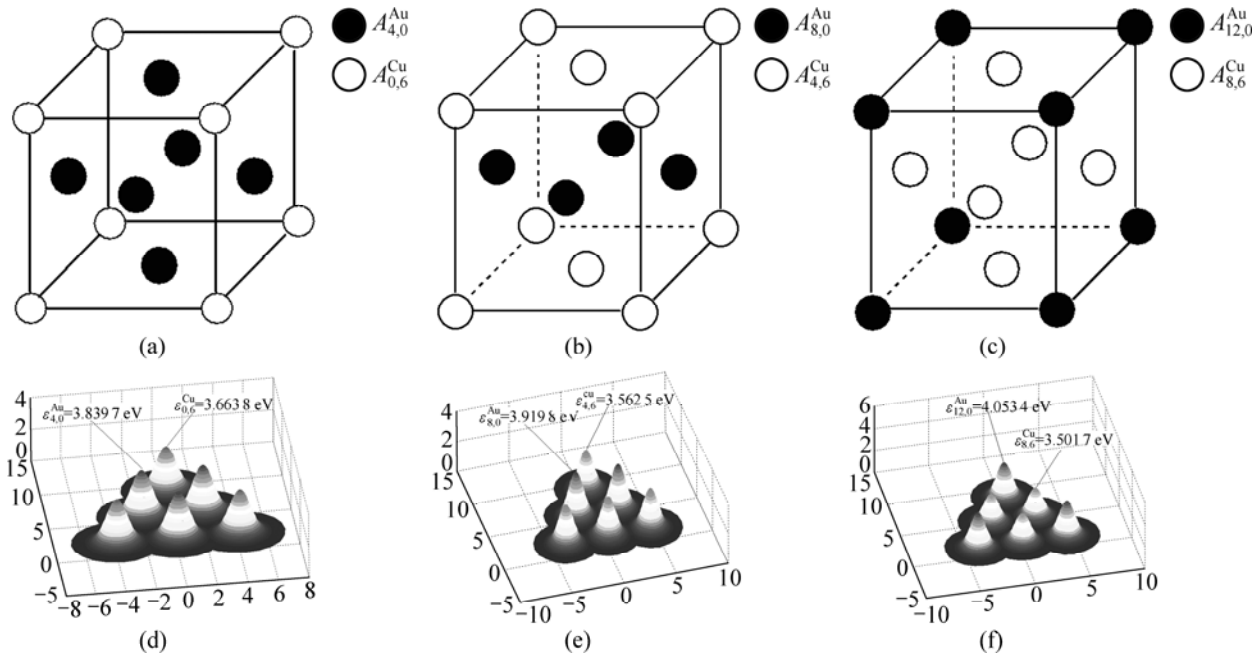

Fig.3 CAO patterns and potential energy wave (111) planes of $L1_2$-Au_3Cu, $L1_0$-AuCu and $L1_2$-$AuCu_3$: (a) $L1_2$-Au_3Cu; (b) $L1_0$-AuCu; (c) $L1_2$-$AuCu_3$; (d) $(\varepsilon^{Au}_{4,0}+\varepsilon^{Cu}_{0,6})-(111)$; (e) $(\varepsilon^{Au}_{8,0}+\varepsilon^{Cu}_{4,6})-(111)$; (f) $(\varepsilon^{Au}_{12,0}+\varepsilon^{Cu}_{8,6})-(111)$

Table 3 Volumetric properties and energetic properties of $L1_2$-Au_3Cu, $L1_0$-AuCu and $L1_2$-$AuCu_3$ compounds as well as corresponding disordered alloys at 298.15 K

Compound	v/(Å^3·atom^{-1})	v_{Au}/(Å^3·atom^{-1})	v_{Cu}/(Å^3·atom^{-1})	Δv^m/(Å^3·atom^{-1})	Δv^m_{Au}/(Å^3·atom^{-1})	Δv^m_{Cu}/(Å^3·atom^{-1})
$L1_2$-Au_3Cu	15.798 7(15.773 1)	16.799 8	12.795 4	0.133 2	−0.152 1	0.988 9
$L1_0$- AuCu	14.514 6(14.447 1)	16.343 7	12.685 5	0.135 4	−0.608 2	0.879 0
$L1_2$-$AuCu_3$	13.162 7(13.105 7)	15.583 4	12.355 9	0.069 9	−1.368 5	0.549 4
$Au_{0.75}Cu_{0.25}$	15.8132	16.845 0	12.718 1	0.147 7	−0.106 9	0.911 6
$Au_{0.5}Cu_{0.5}$	14.5544	16.581 2	12.527 5	0.175 2	−0.370 6	0.721 1
$Au_{0.25}Cu_{0.75}$	13.2079	16.160 7	12.223 7	0.115 1	−0.791 2	0.417 2

Compound	Δv^{ex}/(Å^3·atom^{-1})	Δv^{ex}_{Au}/(Å^3·atom^{-1})	Δv^{ex}_{Cu}/(Å^3·atom^{-1})	Δm_v^{Au}	Δm_v^{Cu}	Δm_v	Δm_v^T	ε/(eV·atom^{-1})
$L1_2$-Au_3Cu	−0.014 5	−0.045 1	0.077 3	0	0	0.095 1	0.095 1	−3.796 8
$L1_0$- AuCu	−0.039 8	−0.237 6	0.157 9	0	0	0.126 0	0.126 0	−3.742 2
$L1_2$-$AuCu_3$	−0.045 2	−0.577 3	0.132 2	0	0	0.092 0	0.092 0	−3.640 7
$Au_{0.75}Cu_{0.25}$	0	0	0	0.003 3	0.001 1	0.048 9	0.051 7	−3.771 6
$Au_{0.5}Cu_{0.5}$	0	0	0	0.004 8	0.004 6	0.069 6	0.074 4	−3.705 5
$Au_{0.25}Cu_{0.75}$	0	0	0	0.003 1	0.008 9	0.055 9	0.063 4	−3.610 8

Compound	ε_{Au}/(eV·atom^{-1})	ε_{Cu}/(eV·atom^{-1})	$\Delta\varepsilon^m$/(eV·atom^{-1})	$\Delta\varepsilon^{ex}_{Au}$/(eV·atom^{-1})	$\Delta\varepsilon^{ex}_{Cu}$/(eV·atom^{-1})	$\Delta m_\varepsilon^{Au}$	$\Delta m_\varepsilon^{Cu}$	Δm_ε
$L1_2$-Au_3Cu	−3.840 8	−3.664 9	−0.065 7	−0.007 9	−0.077 0	0	0	−0.017 4
$L1_0$- AuCu	−3.921 0	−3.563 5	−0.094 0	−0.041 8	−0.031 7	0	0	−0.047 8
$L1_2$-$AuCu_3$	−4.054 6	−3.502 7	−0.075 3	−0.101 5	-0.006 0	0	0	−0.056 8
$Au_{0.75}Cu_{0.25}$	−3.832 9	−3.587 9	−0.040 5	0	0	−0.002 6	−0.001 9	−0.012 2
$Au_{0.5}Cu_{0.5}$	−3.879 2	−3.531 8	−0.057 3	0	0	−0.003 6	−0.003 0	−0.023 4
$Au_{0.25}Cu_{0.75}$	−3.953 1	−3.496 7	−0.045 5	0	0	−0.002 2	−0.002 1	−0.023 7

Compound	Δm_ε^T	E_c/(J·mol^{-1})	ΔH^m/(J·mol^{-1})	ΔV^m/(Å^3·mol^{-1})	a,b/Å	c/Å
$L1_2$-Au_3Cu	−0.017 4	366 335	−6335(−5736)[25]	8.02×10^{22}	3.9832(3.9810)[26]	3.9832(3.9810)[26]
$L1_0$- AuCu	−0.047 8	361 069	−9069(−8746)[25]	8.15×10^{22}	3.9715(3.9662)[27]	3.6808(3.6736)[27]
$L1_2$-$AuCu_3$	−0.056 8	351 268	−7268(−7164)[25]	4.21×10^{22}	3.7480(3.7426)[26]	3.7480(3.7426)[26]
$Au_{0.75}Cu_{0.25}$	−0.014 6	363 904	−3904	8.8957×10^{22}	3.9844	3.9844
$Au_{0.5}Cu_{0.5}$	−0.026 8	357 526	−5526	1.0551×10^{22}	3.8757	3.8757
$Au_{0.25}Cu_{0.75}$	−0.025 9	348 385	−4385	6.9312×10^{22}	3.7523	3.7523

$$\psi(\mathrm{AuCu_3}) = [\mathrm{Xe}](5d_n)^{3.9052}(5d_c)^{5.9793}(6s_f)^{1.1154} + 3[\mathrm{Ar}](3d_n)^{4.6163}(3d_c)^{4.8442}(4s_f)^{1.5394}$$

We have obtained not only the average atomic volumes (v) of these three compounds and corresponding disordered alloys, but also the average atomic volumes (v_{Au} and v_{Cu}) of Au- and Cu-components in Å^3/atom; The average atomic volume of the compound is smaller than that of the corresponding disordered alloy.

We obtained not only the average atomic volumes of formation (Δv^{m}), but also the average atomic volumes of formation ($\Delta v_{\mathrm{Au}}^{\mathrm{m}}$, $\Delta v_{\mathrm{Cu}}^{\mathrm{m}}$) of Au- and Cu-components in Å^3/atom. The average atomic volume of the compound is smaller than that of the corresponding disordered alloy, to which the contribution of the Au-component is negative, the contribution of the Cu-component is positive, and $\Delta v^{\mathrm{m}}>0$.

We have obtained not only the ordering (or excess) average atomic volumes (Δv^{ex}), but also the ordering average atomic volumes ($\Delta v_{\mathrm{Au}}^{\mathrm{ex}}$, $\Delta v_{\mathrm{Cu}}^{\mathrm{ex}}$) of Au- and Cu-components in Å^3/atom, to which the contribution of the Au-component is negative, the contribution of the Cu-component is positive, and $\Delta v^{ex}<0$.

We obtained not only the total average atomic volume mismatch degree (Δm_V^{T}) of these three compounds and corresponding disordered alloys, but also the average atomic volume mismatch degrees (Δm_V) between Au- and Cu-components, as well as their average atomic volume mismatch degrees (Δm_v^{Au}, Δm_v^{Cu}) between characteristic atoms inside the Au- and Cu-components, respectively, in Å^3/atom. The total average atomic volume mismatch degree of the compound is larger than that of the corresponding disordered alloy.

In a similar way to volumetric properties, we obtained the energetic properties: average atomic potential energies (ε, in eV/aton), average atomic potential energies of formation ($\Delta\varepsilon^{\mathrm{m}}$), ordering average atomic potential energies ($\Delta\varepsilon^{\mathrm{ex}}$) and total average atomic potential energies mismatch degrees ($\Delta m_\varepsilon^{\mathrm{T}}$) of these three compounds and corresponding disordered alloys, as well as corresponding energetic properties ($\varepsilon_{\mathrm{Au}}$, $\varepsilon_{\mathrm{Cu}}$; $\Delta\varepsilon_{\mathrm{Au}}^{\mathrm{m}}$, $\Delta\varepsilon_{Cu}^{\mathrm{m}}$; $\Delta\varepsilon_{\mathrm{Au}}^{\mathrm{ex}}$, $\Delta\varepsilon_{\mathrm{Cu}}^{\mathrm{ex}}$; $\Delta m_\varepsilon^{\mathrm{Au}}$, $\Delta m_\varepsilon^{\mathrm{Cu}}$) of Au and Cu components.

We obtained the cohesive energies (E_{c}, in J/mol), heat of formation (ΔH^{m}, in J/mol), volume of formation (ΔV^{m}, in Å^3/mol) and lattice parameters (a, b, c, in Å) of these three compounds and corresponding disordered alloys.

The interpretations of the symbols and units have been given in this section. The experimental values are listed in parentheses.

3.3 Volumetric and energetic properties of AuCuII

3.3.1 CAO pattern of J−L crystalline model

The crystalline structure of AuCuII compound was firstly investigated through X-ray diffractometry by JOHASSON and LINDE[29]. From their results we can know that the AuCuII is a periodic antiphase commensurate structure, stacking of $L1_0$ cells along b equal to 10a, of space group *Imam*, and the number (m) of $L1_0$ cells between two successive antiphase boundary planes is equal to 5. This structure is thus conveniently described as follows: every five order $L1_0$ cells along b axis, an antiphase boundary of vector [1/2 0 1/2] operates, so that after a 10a spacing, the cell is restored (see Fig.4(a1)).

According to J−L model, the CAO pattern has been drawn up (see Fig.4(a2)). It shows that the AuCuII cell consists of two PAD AuCuI regions and two PAD boundary regions. Each PAD AuCuI region contains 6 ($A_{8,0}^{\mathrm{Au}} + A_{4,6}^{\mathrm{Cu}}$) planes perpendicular to b axis, in which the $A_{8,0}^{\mathrm{Au}}$ and $A_{4,6}^{\mathrm{Cu}}$ atoms are arranged alternatively by face center form. Each PAD boundary region contains 4 ($A_{8,1}^{\mathrm{Au}} + A_{4,5}^{\mathrm{Cu}}$) planes, in each plane, the $A_{8,1}^{\mathrm{Au}}$ and $A_{4,5}^{\mathrm{Cu}}$ atoms are arranged alternatively by face center form, the volume and potential energy of each AuCuII cell can be calculated by following equations:

$$V = 12(v_{8,0}^{\mathrm{Au}} + v_{4,6}^{\mathrm{Cu}}) + 8(v_{8,1}^{\mathrm{Au}} + v_{4,5}^{\mathrm{Cu}}) \quad (19)$$

$$E = 12(\varepsilon_{8,0}^{\mathrm{Au}} + \varepsilon_{4,6}^{\mathrm{Cu}}) + 8(\varepsilon_{8,1}^{\mathrm{Au}} + \varepsilon_{4,5}^{\mathrm{Cu}}) \quad (20)$$

The calculated volumetric and energetic properties of PAD AuCuI region are listed in Table 3, and the calculated volumetric and energetic properties of AuCuII and PAD boundary region are listed in Table 4. From Tables 3 and 4, we can obtain following knowledge.

When the AuCuI→AuCuII transformation occurs, the $A_{8,0}^{\mathrm{Au}}$ and $A_{4,6}^{\mathrm{Cu}}$ atoms with higher potential energies ($\varepsilon_{8,0}^{\mathrm{Au}}$ =−3.9210 eV/atom, $\varepsilon_{4,6}^{\mathrm{Cu}}$ =−3.5635 eV/aton) change respectively into the $A_{8,1}^{\mathrm{Au}}$ and $A_{4,5}^{\mathrm{Cu}}$ atoms with lower potential energies ($\varepsilon_{8,1}^{\mathrm{Au}}$ =−3.9255 eV/atom, $\varepsilon_{4,5}^{\mathrm{Cu}}$ =−3.5669 eV/atom) in the PAD boundary region, the transition enthalpy ΔH(AuCuI→AuCuII) is negative (−152.7 J/mol), namely, it is an exothermic reaction, that is opposite from experimental phenomenon.

The $v_{8,1}^{\mathrm{Au}}$ =16.3181 Å^3/atom, which is smaller than $v_{8,0}^{\mathrm{Au}}$ =16.3437 Å/atom, and the $v_{4,5}^{\mathrm{Cu}}$=12.6945 Å^3/atom, which is larger than $v_{4,6}^{\mathrm{Cu}}$ =12.6855 Å^3/atom, but the average atomic volume (14.5113 Å^3) of AuCuII is smaller than the average atomic volume (14.5146 Å^3) of AuCuI, then, the transition volume Δv(AuCuI→AuCuII) is negative (−0.0033 Å^3/atom), that is opposite from the experimental phenomenon too. Therefore, the J−L model can not be used to describe the AuCuII compound.

3.3.2 CAO pattern of G−F−L crystalline model

The in-situ X-ray diffraction experiments and

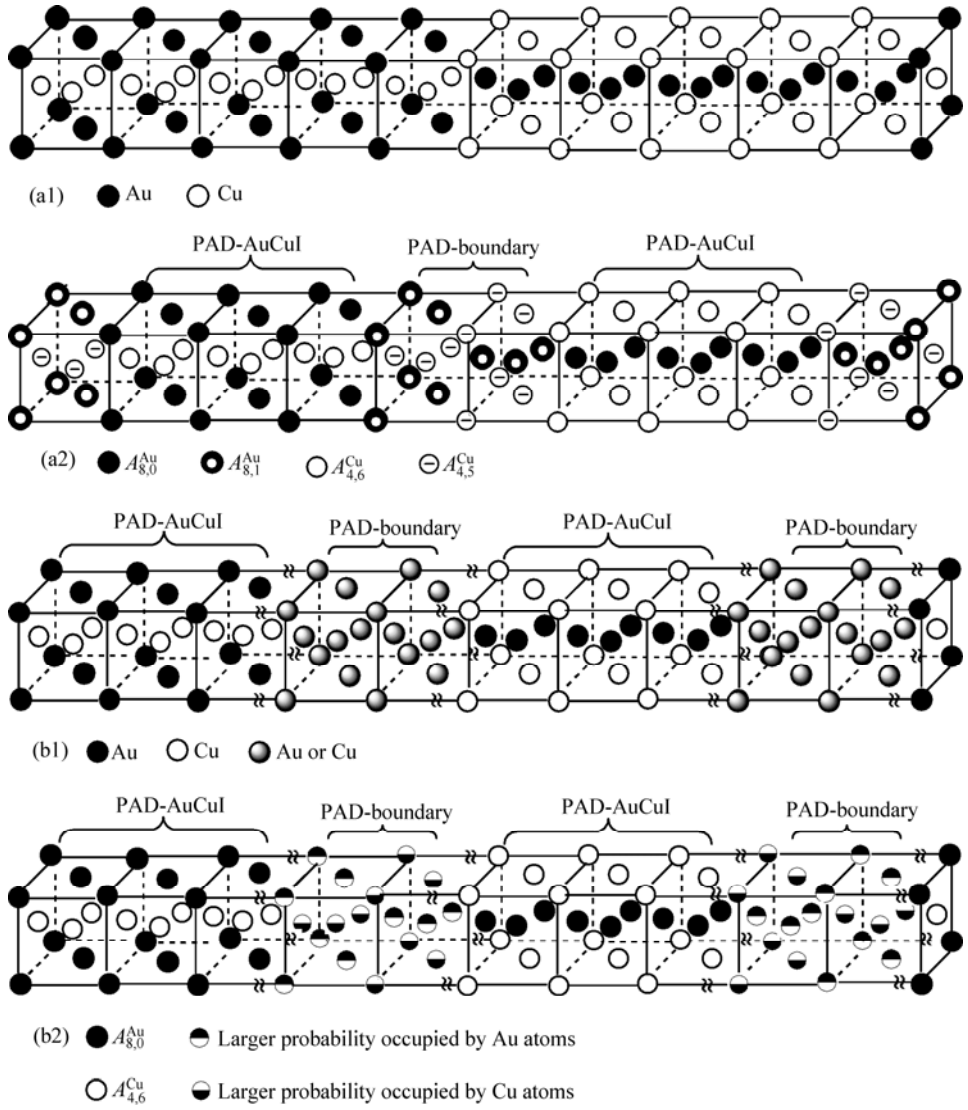

Fig.4 Crystalline structure of J−L model for AuCuII (a1), CAO pattern of J−L model (a2), crystalline structure of G−F−L model (b1) and CAO pattern of G−F−L model (b2)

Table 4 Volumetric properties and energetic properties of AuCuII and PAD boundary(B) region described by J−L model, as well as their transition volumes Δv(AuCuI→AuCuII), Δv(AuCuI→PADB) and transition enthalpy ΔH(AuCuI→AuCuII), ΔH(AuCuI→PADB) (The interpretation of other symbols and units is the same to that of Table 3)

Region	v/(Å^3·atom^{-1})	v_{Au}/Å^3	v_{Cu}/Å^3	ΔV^m/Å^3	ΔV_{Au}^m/Å^3	ΔV_{Cu}^m/Å^3	ΔV^{ex}/Å^3	ΔV_{Au}^{ex}/Å^3	ΔV_{Cu}^{ex}/Å^3	Δv(AuCuI→AuCuII)/Å^3	Δv(AuCuI→PADB)/(Å^3·atom^{-1})
AuCuII	14.5112	16.3334	12.6891	0.1321	−0.6185	0.8826	−0.0431	−0.2478	0.1615	−0.0033	
PADB	14.5063	16.3181	12.6945	0.1271	−0.6338	0.8880	−0.0481	−0.2632	0.1669		−0.0083

Region	ε/(eV·atom^{-1})	ε_{Au}/(eV·atom^{-1})	ε_{Cu}/(eV·atom^{-1})	$\Delta\varepsilon^m$/(eV·atom^{-1})	$\Delta\varepsilon_{Au}^m$/(eV·atom^{-1})	$\Delta\varepsilon_{Cu}^m$/(eV·atom^{-1})	$\Delta\varepsilon^{ex}$/(eV·atom^{-1})	$\Delta\varepsilon_{Au}^{ex}$/(eV·atom^{-1})	$\Delta\varepsilon_{Cu}^{ex}$/(eV·atom^{-1})	ΔH(AuCuI→AuCuII)/(J·mol^{-1})	ΔH(AuCuI→PADB)/(J·mol^{-1})
AuCuII	−3.8155	−3.8511	−3.5649	−0.0956	−0.1087	-0.0825	−0.0383	−0.0436	−0.0330	−152.7	
PADB	−3.7462	−3.9255	−3.5669	−0.0980	−0.1114	-0.0845	−0.0407	−0.0463	−0.0351		−381.8

in-situ temperature observations in transmission electron microscopy on stoichiometric AuCu alloy were performed[28−30]. From their results we can know the follows.

The structure of AuCuII described by G-F-L model is a periodic antiphase incommensurate structure, statistical stacking of $L1_0$ cells along b axis, which is thus periodic along a and c, but only periodic in the

mean along *b*. At the equiatomic composition, AuCuII seems ordered everywhere except in the neighbourhood of the antiphase boundaries (see Fig.4(b1)).

According to CAO pattern of the G−F−L model of the equiatomic AuCuII (see Fig.4(b2)), the AuCuII cell consists of two PAD AuCuI regions and two PAD boundary regions. Each AuCuI region, supposing full order (σ=1), contains m ($A_8^{Au}+A_4^{Cu}$) planes, at the very least m=6, perpendicular to b axis, in which the A_8^{Au} and A_4^{Cu} atoms are arranged alternatively by face center form. Each PAD boundary region contains $m'[(1/x_{Au})\sum_i x_i^{Au}(x,\sigma)A_i^{Au}+(1/x_{Cu})\sum_i x_i^{Cu}(x,\sigma)A_i^{Cu}]$ planes, at the very least m'=4. In each plane, the average $[(1/x_{Au})\sum_i x_i^{Au}(x,\sigma)A_i^{Au}]$ and average $[(1/x_{Cu})\sum_i x_i^{Cu}(x,\sigma)A_i^{Cu}]$ atoms are arranged alternatively by face center form. But the numbers m=6 and m'=4 are nevertheless still the results of an average. The concentrations $x_i^{Au}(x,\sigma)$ and $x_i^{Cu}(x,\sigma)$ of the characteristic atoms A_i^{Au} and A_i^{Cu} are the functions of composition x and ordering degree σ[4], where σ<1. The volume and potential energy of each AuCuII cell described by G−F−L model can be calculated by following equations:

$$V=2m(v_{8,0}^{Au}+v_{4,6}^{Cu})+2m'\cdot((1/x_{Au})\sum_{i=0}^{I}x_i^{Au}(x,\sigma)v_i^{Au}+(1/x_{Cu})\sum_{i=0}^{I}x_i^{Cu}(x,\sigma)v_i^{Cu} \quad (21)$$

$$E=2m(\varepsilon_{8,0}^{Au}+\varepsilon_{4,6}^{Cu})+2m'\cdot((1/x_{Au})\sum_{i=0}^{I}x_i^{Au}(x,\sigma)\varepsilon_i^{Au}+(1/x_{Cu})\sum_{i=0}^{I}x_i^{Cu}(x,\sigma)\varepsilon_i^{Cu}) \quad (22)$$

The calculated results are shown in Fig.5 and listed in Table 5. The experimental ΔH and Δv values are given in the corresponding literatures. From Table 5, we can obtain the following knowledge.

1) Even at the stochiometric AuCu, the transformation AuCuI→AuCuII occurs on a range of transition temperatures, which may be mainly attributed to periodic composition fluctuation in micro-regions. It leads to the diffusion of atoms in cooperation with splitting of the energetic and volumetric states of Au- and Cu-characteristic atoms, to form PADB regions with higher potential energy, larger volume and lower ordering degree, and to make compositional gradient match with both side neighboring PAD AuCuI regions. Therefore, it is an energy absorption and volume expansion reaction, which is consistent with the experimental phenomena.

2) According to potential energies of Au and Cu characteristic atoms, which were determined on the basis of experimental heats of formation of disordered $Au_{1-x}Cu_x$ alloys in the compositional ranges $0\le x_{Cu}\le 25\%$ and $75\%\le x_{Cu}\le 100\%$ to avoid effect of short-range (SR) ordering degree, the transition enthalpy ΔH of transformation AuCuI→AuCuII as functions of average ordering degree σ of AuCuII and σ(PADB) of the PADB region are calculated. According to experimental transition enthalpies 325.6, 756.1 and 886.5 J/mol, their corresponding ordering degrees of the PADB regions are respectively 0.878, 0.683 and 0.621. If taking m=9 and m'=4, their ordering degrees of the PADB regions decrease, but their average ordering degrees of AuCuII keep consistent.

3) According to the volumes of Au and Cu characteristic atoms obtained from experimental volumes

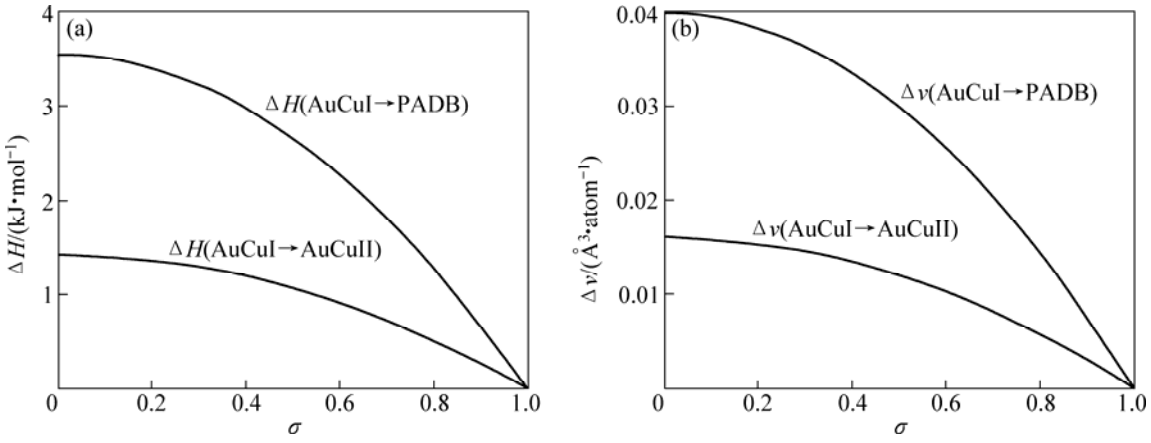

Fig.5 Calculated ΔH(AuCuI→AuCuII), Δv(AuCuI→AuCuII) as function of ordering degree σ(AuCuII) for transition AuCuI→AuCuII, as well as ΔH(AuCuI→PADB), Δv(AuCuI→PADB) as function of ordering degree σ(PADB) for transition AuCuI→PADB region at equiatomic AuCu, when AuCuI region has full order, m=6 and m'=4. Here σ denotes σ(AuCuII) for AuCuII or σ(PADB) for PADB region, respectively

Table 5 Transition enthalpy ΔH(AuCuI→AuCuII) and transition volume Δv(AuCuI→AuCuII) and transition average lattice constant Δa(AuCuI→AuCuII) as functions of average ordering degree σ(AuCuII) of AuCuII and ordering degree σ(PADB) of PADB region, when AuCuI region has full order, as m=6, m'=4 and m=9, m'=4

m=6, m'=4					m=9, m'=4				
σ(AuCuII)	σ(PADB)	ΔH/(J·mol^{-1})	Δv/(Å^3·atom^{-1})	Δa/Å	σ(AuCuII)	σ(PADB)	ΔH/(J·mol^{-1})	Δv/(Å^3·atom^{-1})	Δa/Å
1	1	0	0	0	1	1	0	0	0
0.961	0.9	269	0.0030	0.0003	0.970	0.9	207	0.0023	0.0002
0.953	0.878	325[28]	0.0036	0.0003	0.953	0.838	325[28]	0.0036	0.0003
0.925	0.8	510	0.0057	0.0005	0.943	0.8	392	0.0044	0.0004
0.892	0.7	722	0.0081	0.0007	0.918	0.7	555	0.0062	0.0006
0.887	0.683	756[31]	0.0085	0.0008	0.896	0.6	697	0.0078	0.0007
0.866	0.621	886[32]	0.0100	0.0009	0.887	0.554	756[31]	0.0085	0.0008
0.863	0.6	906	0.01020	0.0009	0.877	0.5	817	0.0092	0.0008
0.837	0.5	1062	0.0119	0.0011	0.866	0.432	886[32]	0.0099	0.0009
0.815	0.4	1190	0.0134	0.0012	0.861	0.4	915	0.0103	0.0009
0.798	0.3	1289	0.0145	0.0013	0.849	0.3	991	0.0111	0.0010
0.792	0.260	1321	0.0149[28]	0.0013	0.839	0.2	1046	0.0118	0.0010
0.785	0.2	1360	0.0153	0.0014	0.834	0.1	1079	0.0121	0.0011
0.777	0.1	1402	0.0158	0.0014	0.832	0	1090	0.0123	0.0011
0.775	0	1417	0.01593	0.0014					

of disordered $Au_{1-x}Cu_x$ alloys, the transition volume Δv of transition AuCuI→AuCuII as functions of average ordering degree σ of AuCuII and σ(PADB) of the PADB region are calculated and also listed in Table 5. According to experimental transition volume of 0.0149 Å/atom, the calculated ordering degrees σ(PADB) is 0.260, which is much smaller than those obtained from experimental transition enthalpies. If the volumes of Au and Cu characteristic atoms are determined on the basis of experimental volumes of $L1_2$-Au_3Cu, $L1_0$-AuCu and $L1_2$-$AuCu_3$ compounds, the calculated ordering degree σ(PADB) is 0.569, which is close to 0.593 obtained by experimental transition enthalpy of 886.5 J/mol. This fact tells us that there is effect of SR ordering degree on the volumes of Au and Cu characteristic atoms obtained from experimental volumes of disordered $Au_{1-x}Cu_x$ alloys in the whole composition range.

4) In the range of AuCuI→AuCuII transition temperatures, the disorder should spread PAD-AuCuI region with high ordering degree $\sigma(H)$ and PADB region with low ordering degree $\sigma(L)$. From Eqs.(21) and (22), it can be known that the property q denoting v and ε can be calculated by the following equation, which is a function of composition x, temperature T and ordering degree σ:

$$q = 2m\left((1/x_{\mathrm{Au}})\sum_{i=0}^{I} x_i^{\mathrm{Au}}(x,\sigma(H))q_i^{\mathrm{Au}} + (1/x_{\mathrm{Cu}})\sum_{i=0}^{I} x_i^{\mathrm{Cu}}(x,\sigma(H))q_i^{\mathrm{Cu}}\right) + 2m'\left((1/x_{\mathrm{Au}})\sum_{i=0}^{I} x_i^{\mathrm{Au}}(x,\sigma(L))q_i^{\mathrm{Au}} + (1/x_{\mathrm{Cu}})\sum_{i=0}^{I} x_i^{\mathrm{Cu}}(x,\sigma(L))q_i^{\mathrm{Cu}}\right) \quad (23)$$

4 Conclusions

1) According to the potential energies and volumes of characteristic atoms separated from the experimental formation heats and lattice constants of disordered $Au_{1-x}Cu_x$ alloys, the electronic structures, potential energy curves lattice constants, cohesive energies and Debye temperatures of corresponding characteristic crystals were obtained, and the nature of variations of their potential energies and volumes with the numbers of Cu-atoms in the neighboring configurations was expounded. The electronic structures of the primary characteristic Au and Cu crystals, i.e., pure fcc Au and Cu metals, obtained by VB theory and EB theory (LRC and LMTO methods) were compared. They are approaching each to each. But the electronic structures of other characteristic crystals (atoms) cannot be obtained by EB theory. Therefore, the VB theory of characteristic crystals has enriched contents of electronic structure theory of alloys.

2) According to CAO patterns of observed $L1_2$-Au_3Cu, $L1_0$-AuCu and $L1_2$-$AuCu_3$ compounds: the electronic structures, potential energies and volumes of Au and Cu atoms at each lattice point in these compounds; the total electronic structures, total volumes,

total potential energies (cohesive energies), total volumes of formation and total enthalpies of formation, total ordering volumes and total ordering enthalpies of these compounds; as well as the corresponding energetic and volumetric properties of Au and Cu components.

3) The CAO pattern of J−L model shows that the transition AuCuI→AuCuII is an exothermic volume contraction reaction, which is opposite from experimental phenomena. The CAO pattern of G−F−L model can be used to explain the structure of AuCuII and to calculate energetic and volumetric properties, and ordering degrees of the PADB region, PAD AuCuI region and AuCuII phase, if there are precise experimental values of enthalpies and volumes of transition AuCuI→AuCuII.

References

[1] XIE You-qing. Atomic energies and Gibbs energy functions of Ag-Cu alloys [J]. Science in China: Series E, 1998, 41: 146−156.

[2] XIE You-qing, ZHANG Xiao-dong. Atomic volumes and volumes functions of Ag-Cu alloys [J]. Science in China: Series E, 1998, 41: 157−168.

[3] XIE You-qing, ZHANG Xiao-dong. Electronic structure of Ag-Cu alloys [J]. Science in China (series E), 1998, 41: 225−236.

[4] XIE You-qing, ZHANG Xiao-dong. Phase diagram and thermodynamic properties of Ag-Cu alloys [J]. Science in China: Series E, 1998, 41: 348−356.

[5] XIE You-qing, TAO Hui-jing, PENG Hong-jian, LI Xiao-bo, LIU Xin-bi, PENG Kun. Atomic states, potential energies, volumes, stability and brittleness of ordered FCC $TiAl_2$ type alloys [J]. Physica B, 2005, 366: 17−37.

[6] XIE You-qing, PENG Hong-jian, LIU Xin-bi, PENG Kun. Atomic states, potential energies, volumes, stability and brittleness of ordered FCC Ti_3Al-type alloys [J]. Physica B, 2005, 362: 1−17.

[7] XIE You-qing, LIU Xin-bi, PENG Kun, PENG Hong-jian. Atomic states, potential energies, volumes, stability and brittleness of ordered FCC $TiAl_3$-type alloys [J]. Physica B, 2004, 353: 15−33.

[8] XIE You-qing, PENG Kun, LIU Xin-bi. Influences of x_{Ti}/x_{Al} on atomic states, lattice constants and potential energy planes of ordered FCC TiAl-type alloys [J]. Physica B, 2004, 344: 5−20.

[9] LUPIS C P P. Chemical thermodynamics of materials [M]. Amsterdam, North-Holland, 1983: 438−469.

[10] SUNDMAN B, FRIES S G, OATES A W. A thermodynamic assessment of Au-Cu system [J]. CALPHAD, 1998, 22(3): 335−354.

[11] KIKUCHI R. A theory of cooperative phenomena [J]. Phys Rev, 1951, 81: 988−1003.

[12] ASTA M, WOLVERTON C, FONTAINE D, DREYSSÉ H. Effective cluster interactions from cluster-variation formalism. I [J]. Phys Rev B, 1991, 44: 4907−4913.

[13] ASTA M, WOLVERTON C, FONTAINE D, DREYSSÉ H. Effective cluster interactions from cluster-variation formalism. II [J]. Phys Rev B., 1991, 44: 4914−4924.

[14] OZOLINš V, WOLVERTON C, ALEX Z. Cu-Au, Ag-Au, Cu-Ag and Ni-Au intermetallics: First-principles study of temperature-composition phase diagrams and structure [J]. Phys Rev B, 1998, 57: 6427−6442.

[15] XIE You-qing, LI Xiao-bo, LIU Xin-bi, PENG Hong-jian, NIE Yao-zhuang. Potential energy sequences of characteristic atoms on basis of heats of formation of disordered $Au_{(1-x)}Cu_x$ alloys(I) [J]. Journal of Materials Science and Engineering, 2009, 3(3): 51−68.

[16] XIE You-qing, LIU Xin-bi, LI Xiao-bo, PENG Hong-jian, NIE Yao-zhuang. Potential energy sequences of characteristic atoms on basis of heats of formation of disordered $Au_{(1-x)}Cu_x$ alloys(Part 2) [J]. Journal of Materials Science and Engineering, 2009, 3(6): 44−57.

[17] XIE You-qing, LI Xiao-bo, LIU Xin-bi, PENG Hong-jian, NIE Yao-zhuang. Volume sequences of characteristic atoms separated from experimental volumes of disordered $Au_{(1-x)}Cu_x$ alloys [J]. Journal of Materials Science and Engineering, 2009, 3(10): 54−75.

[18] PAULING L. The nature of the chemical bond [M]. third edition. Ithaca: Cornell University Press, 1960.

[19] XIE You-qing, ZHANG Xiao-dong, ZHAO Li-ying, Ma Xiu-lin. Electronic structure and properties of pure copper [J]. Science of China A, 1993, 36: 487−496.

[20] XIE You-qing, ZHANG Xiao-dong, MA Xiu-lin, ZHAO Li-ying. Electronic structure and properties of pure gold [J]. Trans Nonferrous Met Soc China, 1992, 2(1): 56−62.

[21] XIE You-qing. Electronic structure and properties of pure iron [J]. Acta Metall Mater, 1994, 42(11): 3705−3715.

[22] XIE You-qing, MA Liu-ying. The theoretical lattice parameters for valence electron structure of crystals [J]. J Cent South Inst Min Metall, 1985(1): 1−9. (in Chinese)

[23] XIE You-qing. A new potential function with many-atom interactions in solid [J]. Science in China A, 1993, 36: 90−98.

[24] ECKARDT H, FRITSCHE L, NOFFKE J J. Self-consistent relativistic band structure of the noble metal [J]. J Phys F: Met Phy, 1984, 14(1): 97−112.

[25] HULTGREN R, DESAI P D, HAWKINS DT, GLEISER M, KELLEY K K. Selected values of thermodynamic properties of binary metals and alloys [M]. Metal Park, OH: American Society for Metals, 1973.

[26] BHATA M L, CAHN R W. Lattice parameter and volume changes on disordering [J]. Intermetallics, 2005, 13(5): 474−483.

[27] JOHANNSSON C H, LINDE J O. Roentgenographic and electrical investigations of the Cu-Au system [J]. Ann Phys, 1936, 25: 1−48.

[28] FEUTELAIS Y, LEGENDRE B, GUYMONT M. New enthalpies determination and in situ X-ray diffraction observations of order/disorder transitions in $Au_{0.5}Cu_{0.5}$ [J]. Acta Mater, 1999, 47(8): 2539−2551.

[29] BONNEANX J, GUYMONT M. Study of the order-disorder transition series in AuCu by in-situ temperature electron microscopy [J]. Intermetallics, 1999, 7(7): 797−805.

[30] GUYMONT M, FEUTELAIS Y, LEGENDRA B. Phase transitions in $Au_{0.5}Cu_{0.5}$ [J]. J Phys IV France, 2001, 11(10): 103−107.

[31] ORIANI R A, MURPHY W K. Thermodynamics of ordering alloys-III Energies of transformation of the AuCu phases [J]. J Phys Chem Solids, 1958, 6(2−3): 277−279.

[32] TISSOT P, DALLENBACH R. THERMOCHIM. Study of order—Disorder transformation of copper-gold alloys by means of differential thermal analysis [J]. Thermochimica Acta, 1978, 25(2): 143−153.

以无序合金的实验数据为基础的 Au_3Cu，$AuCu_3$，AuCuI 和 AuCuII 的特征原子占据图

谢佑卿[1, 2, 3]，李艳芬[1, 2, 3]，刘心笔[1, 2, 3]，李晓波[4]，彭红建[1, 2, 3]，聂耀庄[1, 2, 3]

1. 中南大学 材料科学与工程学院，长沙 410083；
2. 中南大学 粉末冶金研究院，长沙 410083；
3. 中南大学 粉末冶金国家重点实验室，长沙 410083；
4. 湘潭大学 机械工程学院，湘潭 411105

摘 要：根据无序 $Au_{1-x}Cu_x$ 合金的实验生成热和晶格常数得到只考虑近邻原子组态的特征原子的势能、体积和电子结构，计算 $L1_2$-Au_3Cu, $L1_2$-$AuCu_3$ 和 $L1_0$-AuCu 化合物的特征原子占据(CAO)图、电子结构、能量和体积性质。Johasson−Linde(J−L)模型的 CAO 图表明，AuCuI→AuCuII 转变是一个放热且体积缩小的反应，但正好与实验现象相反。根据 Guymont−Feutelais−Legendre(G−F−L)模型的 CAO 图，AuCuII 晶胞由两个周期反相(PAD)的 AuCuI 区域和两个 PAD 边界区域组成；从 G−F−L 模型的 CAO 图得出的公式可用来计算 PAD AuCuI 区域和 PAD 边界区域的能量性质、体积性质和有序度及 AuCuII 相的平均性质，计算结果与实验现象相吻合。

关键词：Au-Cu 系；金属间化合物；电子结构；晶体结构；特征原子占据图

(Edited by YANG Hua)